MRS. LAURI L SADORUS (Orcid ID : 0000-0003-0084-9381)

DR. JOSEP V. PLANAS (Orcid ID : 0000-0002-6525-9617)

Article type : Original Article

TITLE

Multiple life-stage connectivity of Pacific halibut (*Hippoglossus stenolepis*) across the Bering Sea and Gulf of Alaska

SHORT TITLE

Ocean basin connectivity of Pacific halibut

AUTHORS

Lauri L. Sadorus[1], Esther D. Goldstein[2], Raymond A. Webster[1], William T. Stockhausen[2], Josep V. Planas[1], and Janet T. Duffy-Anderson[2]

[1] International Pacific Halibut Commission, Seattle, Washington, U.S.A.

[2] National Marine Fisheries Service, National Oceanic and Atmospheric Administration, Alaska Fisheries Science Center, Seattle, Washington, U.S.A.

CORRESPONDENCE

Lauri L. Sadorus
International Pacific Halibut Commission, 2320 W Commodore Way, Suite 300, Seattle, Washington 98199
Email: Lauri.sadorus@iphc.int

ACKNOWLEDGMENTS

We are grateful to all of the vessel crews and field biologists for their efforts in collecting the data used in this analysis and to parameterize the models. We would like to thank NOAA scientists Dan Cooper and Dr. Gerald Hoff, and IPHC scientists Dr. Piera Carpi, Dr. Timothy Loher and Dr. Ian Stewart, for their helpful advice and reviews of the manuscript. We also thank the two anonymous reviewers who helped to strengthen the manuscript. The scientific views, opinions, and conclusions expressed herein are solely those of the authors and do not represent the views, opinions, or conclusions of NOAA or the Department of Commerce. This is FOCI Contribution Number EcoFOCI-N955.

CONFLICT OF INTEREST

The authors declare that there is no conflict of interest regarding the publication of this article.

DATA AVAILABILITY STATEMENT

The data that support the findings of this study are openly available in the Ichthyoplankton Information System Database (https://access.afsc.noaa.gov/ichthyo/), the Alaska Groundfish Bottom Trawl Survey Data database, (https://www.fisheries.noaa.gov/alaska/commercial-fishing/alaska-groundfish-bottom-trawl-survey-data), and through the International Pacific Halibut Commission upon request at https://www.iphc.int/form/data-request .

ABSTRACT

Pacific halibut (*Hippoglossus stenolepis*) is managed as a single stock throughout the Gulf of Alaska (GOA) and eastern Bering Sea (BS), but biogeographical barriers and the potential for differential impacts of climate change may alter habitat use and distributions, and restrict connectivity between these ecosystems. To improve our understanding of larval dispersal pathways and migrations of young fish within and between GOA and BS, we (1) examined potential pelagic larval dispersal and connectivity between the two basins using an individual-based biophysical model (IBM) focusing on years with contrasting climatic conditions, and (2) tracked movement of fish up to age-6 years using annual age-based distributions and a spatio-temporal modeling approach. IBM results suggest that the Aleutian Islands constrain connectivity between GOA and BS, but that large island passes serve as pathways between these ecosystems. The degree of connectivity between GOA and BS is influenced by spawning location such that an estimated 47-58% of simulated larvae from the westernmost GOA spawning location arrived in the BS, with progressive reductions in connectivity from spawning grounds further east. From the results of spatial modeling of 2-6 year old fish, we can infer ontogenetic migration from the inshore settlement areas of eastern BS towards Unimak Pass and GOA. The pattern of larval dispersal from GOA to BS, and subsequent post-settlement migrations back from BS toward GOA, provides evidence of circular, multiple life-stage, connectivity between these ecosystems, regardless of climatic variability or year class strength.

KEYWORDS

Bering Sea, population connectivity, Gulf of Alaska, juvenile, larvae, migration, Pacific halibut, larval dispersal

INTRODUCTION

The Pacific halibut (*Hippoglossus stenolepis*) population in North American waters of the Pacific Ocean and Bering Sea (BS) supports vibrant commercial, recreational, subsistence, and tribal fisheries. The management strategy in Alaskan waters encompasses both the Gulf of Alaska (GOA) and the BS and uses stock assessment models of spawning biomass combined with agreed management approaches (Stewart & Hicks, 2018) to manage the species as a single, panmictic population, although the International Pacific Halibut Commission (IPHC) also uses

current stock distribution to inform harvest distribution. Despite this cross-ecosystem management strategy, the Aleutian Islands are a permeable barrier between the North Pacific and BS ecosystems (Seitz et al., 2011; Spies, 2012; Parada et al., 2016), and there is evidence of differential impacts of climate change across these marine ecosystems such as loss of sea ice in the BS, warm and cold temperature stanzas in the BS (Duffy-Anderson et al., 2017), and warming events in the GOA (Cavole et al., 2016). Such ecosystem discontinuities have the potential to impact species that rely on large geographic domains and multiple habitats throughout their life cycles (Norcross et al., 1999; Mumby et al., 2004; Rochette et al., 2010). For Pacific halibut, fluctuations in year class strength may be determined by conditions during the early life stages that influence growth, survival, and transport to suitable habitats (Bailey et al., 2005). Population age composition of Pacific halibut indicates that a single large year class can dominate the fishery for several years (Stewart & Hicks, 2018), implying that environmental conditions that influence year class strength can have lasting impacts on fishery yield.

Pacific halibut have a complex life-cycle with passive dispersal and active migration stages, and there is evidence to suggest that connectivity between the GOA and BS may occur across multiple life stages. Adults spawn during winter in the deep water of the outer continental shelf and slope throughout the GOA and BS (Thompson & Van Cleve, 1936; Skud, 1977; Sohn et al., 2016). Dispersal occurs during the pelagic egg and larval stages, and after ~5-7 months, once metamorphosis into the asymmetrical adult form is complete, the juvenile settles to inshore shallow nursery areas (St. Pierre, 1989; Thompson & Van Cleve, 1936). Oceanographically-driven connectivity between the GOA and BS is primarily unidirectional, and fish that are spawned in the GOA may be exported into the BS through Aleutian Island passes (Best, 1977; Skud, 1977; Hinckley et al., 2019). However, mark-recapture studies show that some Pacific halibut during the juvenile and adult life stages migrate from the BS into the GOA (Dunlop et al., 1964; Webster et al., 2013), counteracting the assumed prevailing direction of larval transport. This potential circular transport and migration pathway suggests cross-ecosystem dependence and reliance on habitats in both the GOA and the BS during different life-stages.

Ecosystem changes such as shifts in oceanography (Stabeno et al., 2012), warm and cold climate stanzas, loss of sea ice, and declines in high quality food in the BS (Kimmel, 2018; Duffy-Anderson et al., 2017; Duffy-Anderson et al., 2019) can create survival bottlenecks for species that transition between ecosystems. For example, egg and larval distributions are

influenced by the strength and direction of ocean currents that vary among temperature regimes (Stabeno et al., 2012) and seasons (Stabeno et al., 2002; 2016a; 2016b). Shifts in oceanographic currents can profoundly influence the survival of eggs and larvae through favorable transport to hospitable habitats that support growth and survival (Goldstein et al. 2020; Bailey & Picquelle, 2002; Atwood et al., 2010; Napp et al., 2000; Petitgas et al., 2013). Movement by young juveniles, however, is not dictated by oceanographic currents to the same degree as larval dispersal, and there is evidence for counter-current migrations of Pacific halibut (Skud, 1977; St. Pierre, 1989; Clark & Hare, 1998; Webster et al., 2013). Thus, a multiple life-stage approach is required to assess the degree of connectivity between the GOA and the BS and the reliance of Pacific halibut populations on both ocean basins.

Identifying population connectivity across marine ecosystems that incorporates both larval dispersal and active migration could aid in the development of holistic management strategies that reflect habitat requirements across life stages as well as factors that contribute to year class strength. To better understand the geographic continuity of Pacific halibut populations and the vulnerabilities of Pacific halibut to environmental change, we assess life stage-specific distributions and connectivity between the GOA and the BS during years of warm and cold temperature stanzas and opposing year class strength using, (1) empirical larval distributions, (2) an individual-based biophysical larval dispersal model, and (3) spatio-temporal modeling of age-specific data. Incorporating larval dispersal and subsequent ontogenetic migration will provide a holistic understanding of population connectivity, multi-life stage habitat use, and potential vulnerabilities of the Pacific halibut fishery to ecosystem change.

MATERIALS AND METHODS

Geographic area

The geographic area for this analysis includes the GOA and BS (Figure 1). Within the GOA, the westward flowing Alaskan Stream is the primary water source for flow through multiple Aleutian Island passes connecting the GOA and BS ecosystems (Royer, 1981; Reed & Schumacher, 1986; Stabeno et al., 1995). Originating in the central GOA is the Alaska Coastal Current (ACC) which flows westward along the continental shelf (Stabeno et al., 1999) and is the primary source for flow through Unimak Pass which is the first major pass encountered by the westward flowing current and also the only major connection point between the BS and GOA

continental shelves. Based on drifter trajectories, after entering the BS via Unimak Pass, water then flows along the 50-m, 100-m, and 200-m isobaths to the west and north in the BS (Stabeno et al., 2002).

Catch data

Larval catch and effort data were obtained from the National Oceanic and Atmospheric Administration (NOAA) Alaska Fishery Science Center Ichthyoplankton Information System database (https://access.afsc.noaa.gov/ichthyo/; NOAA 2019). Gear used for data collection most often included a MARMAP (Marine Resources Monitoring, Assessment and Prediction program) type bongo sampler (Posgay & Marak, 1980) with an inside diameter of 60 cm and a 0.333 or 0.505-mm mesh net. Tucker trawl gear was used less often and was composed of cone-shaped fine-mesh nets. Bongo and Tucker gear were determined to fish the same population (Boeing & Duffy-Anderson, 2008) and standardized catches are therefore considered comparable for analysis. Pacific halibut larvae were identified and catches for both gears were standardized to number of individuals caught under 10 m^2 of sea surface area (Smith & Richardson, 1977).

For juvenile and adult fish analyses, catch and effort data from the NOAA Alaska Fisheries Science Center summer bottom trawl survey (NOAA 2020), were coupled with individual fish information, including ages derived from otoliths collected during the surveys (age data available upon request https://www.iphc.int/form/data-request). The NOAA BS bottom trawl survey was conducted annually with stations located on a 20 nautical mile square grid extending from inner Bristol Bay in the eastern BS within the 200-m depth contour (Figure 1). The standard survey trawl gear and survey design are described in Stauffer (2004) and Clark et al. (1997). The GOA bottom trawl survey was conducted biennially and consisted of a stratified random sampling design based on data from previous surveys (Stauffer, 2004; Clark et al., 1997). Gear for this survey is described in Stauffer (2004). Net mensuration systems recorded net performance, and electronic data loggers recorded temperature and depth during both surveys. Area-swept catch per unit effort was calculated from the distance towed and net width (Clark et al., 1997). Once settled, Pacific halibut are not routinely monitored until they are captured during the NOAA Alaska Fisheries Science Center summer bottom trawl surveys at 2 years of age. From various studies it has been observed that age-0 and age-1 Pacific halibut reside in bays and inshore waters from Dixon Entrance to Unimak Pass in the GOA and along the Alaska Peninsula and

Bristol Bay in the BS (Best & Hardman, 1982; Norcross et al., 1997; Best, 1977; Stoner & Abookire, 2002). Occasionally, age-1 fish have been caught in the bottom trawl survey, but that number is small, and those in the aging sample and confirmed as age-1 fish, totaled just 57 individuals from 2000-2018 according to the IPHC database. Due to the low numbers of these age-0 and age-1 fish, and lack of standardized monitoring, estimates of relative abundance and modeling of distribution begin at age 2. Thus, catch data from the 2007-2015 bottom trawl surveys were used to examine 2-6 year old fish.

Age data

Age in whole years (2-6 year olds) for demersal juveniles was established using right sagittal otoliths collected during the NOAA Alaska Fisheries Science Center summer bottom trawl surveys. In younger fish (< 5 years), otoliths were surface-aged, i.e. annuli counted on the surface using dissecting microscopes. In older fish or if annuli were indistinct, the break and bake method of aging (described in Forsberg, 2001) was used. While not all trawl stations have Pacific halibut age data collected, the spatial coverage of aged fish was generally comprehensive for the cohorts examined here, particularly in the BS. Although coverage in the biennial GOA survey had some gaps, these were not sufficient to affect our interpretation of the overall distributional patterns.

Cohorts studied

The 2005 and 2009 Pacific halibut year classes were selected as focal cohorts for analysis based on the following rationale: (1) they represent cohorts spawned during distinct BS environmental stanzas (i.e. warm and cold, respectively) (Stabeno et al., 2012), (2) they represent relatively strong and weak year classes, respectively (Stewart & Hicks, 2018), and, 3) the sampling coverage at both the pelagic and settled phases for the two selected cohorts was robust and comparable. The supplemental year classes of 2003, 2004, 2010, and 2011 were added to the larval dispersal modeling and to the subsequent spatio-temporal modeling of older life stages to contrast patterns and strengthen comparisons of advection and migration during warm and cold years. For analytical purposes involving annual cohort analyses, one hatch date (January 1) is assigned per spawning season, regardless of actual spawn date to assign year classes. For

example, the 2005 year class includes those larvae spawned from Autumn 2004 through Spring 2005.

Individual-based biophysical model

Larval dispersal, transport, and connectivity were determined using a three dimensional individual based biophysical model (IBM) coupled with daily-averaged output from a hydrodynamic model (ROMS, https://www.myroms.org/). The IBM was developed using the Dispersal Model for Early Life Stages (DisMELS) IBM framework (Stockhausen et al. 2019a) to track transport and dispersal of the pelagic egg and larval stages of marine organisms through earlier life stages from spawning to settlement. Briefly, DisMELS incorporates a Lagrangian particle tracking algorithm and species-specific traits, allowing the model to be parameterized for multiple species (Stockhausen et al., 2019b; Duffy-Anderson et al., 2013; Cooper et al., 2013; Sohn, 2016). The hydrographic ROMS model is a primitive equation, three dimensional ocean circulation model driven by atmospheric forcing (details are available at: myroms.org, Shchepetkin & McWilliams, 2005; Haidvogel et al., 2008). The ocean model used for the present study was the regional Northeast Pacific ROMS model (NEP 6) with ~10 km resolution that spans the GOA and the BS. NEP 6 incorporates sea ice and tidal dynamics that are important for circulation within the study region (Danielson et al., 2011; Hermann et al., 2013) and has previously been utilized for larval dispersal models in the BS (Petrik et al., 2016). Output from the ROMS model was saved in daily increments. For the IBM, ROMS daily output was spatially interpolated using bilinear interpolation in order to obtain the physical variables associated with each modeled larvae. Larval locations (latitude, longitude, and depth) were determined using a fourth-order predictor-corrector algorithm that incorporated swimming, buoyancy, and vertical and horizontal random walks for diffusive motion (Stockhausen et al., 2019b). Larval movement was primarily passive (no orientation or directed swimming behavior) except for vertical movement to maintain larvae within preferred depth ranges (Table 1). Larval locations as well as age, size, and development stage were based on 20-minute time steps and saved at daily time steps.

Pacific halibut larval release locations for the IBM were based on known spawning locations (St. Pierre, 1989) that were manually-digitized to create spatial polygons that contained point locations with a 1-km resolution grid for simulated larval release (ESRI ArcMap version 10.6;

Figure 2), and were the same for all modelled years. A total of 200 individuals were released from each grid cell. Pacific halibut typically spawn from October-April; however, the exact monthly spawn dates are unknown. Therefore, larvae were released from October-April during each study year from the 25th-28th of each month at midnight to capture the general monthly dispersal patterns. Larval early life history traits generally followed those described in Sohn (2016) and larval mortality was not included in the model. Based on limited nursery habitat information throughout the study domain, all model simulations were terminated once a larvae reached the newly-settled juvenile stage after a pelagic larval duration of 180 days (Table 1). This time- and stage-based model termination limits conclusions that can be made regarding settlement success and post-settlement survival, but provides insight regarding dispersal distance.

Spatio-temporal model

Spatial modeling of trawl survey data allows for a more expansive (but less direct) assessment of cohort movement patterns than is possible using common wire tagging mark-recapture methods. Modeling the 2005 and 2009 year classes provides a look at the similarities and differences between relatively strong and weak cohorts that were spawned during warm and cold environmental stanzas, respectively. Data from other cohorts of intermediate strength (2003-04 and 2010-11 year classes) were also modeled, with results available in supplementary material.

All Pacific halibut caught during the trawl surveys were measured to obtain length data, but spatial coverage for age sampling was often less extensive. To overcome these data limitations, a spatio-temporal modeling approach was utilized (Webster et al., 2020) in order to leverage information about spatial and temporal dependence from observed data to make predictions of abundance within habitat that is unsampled in a given year, as well as improve the quality of estimation elsewhere. For each spatial location (i.e., trawl survey station), the catch-per-unit-effort (CPUE) was computed by dividing catch weight for fish with known age by survey station effort (net width times tow distance), and then adjusting for the sampling fraction in cases where less than 100% of fish were aged. For each aged cohort at each survey station in each year:

$$CPUE = \frac{W}{E} * (\frac{1}{f}) \quad (1)$$

where W=catch weight of fish, E=effort (net width x distance) and f=sampling fraction of halibut (proportion aged).

In summary, let $c(s,t)$ be the trawl CPUE value of a given cohort at location s and year t, where s represents the spatial locations of the fished survey stations, taking values $s_1, \ldots, s_n$ and $t = t_1, \ldots, t_T$, corresponding to ages 2 to (T+1). In this model, $s_i \in S^2$, the set of points on the surface of a sphere, and therefore coordinates in longitude and latitude format are converted to Cartesian coordinates on a sphere for modeling. Data from the trawl surveys contain observations of zero CPUE, due to stations in low-density areas catching no Pacific halibut. The probability that $c(s,t)=0$ is accounted for by using a semi-continuous model, which models the data as a combination of zero and non-zero processes. Two new variables are defined, $x(s,t)$ for presence or absence of Pacific halibut in the catch, and $y(s,t)$ for the CPUE value when Pacific halibut are present:

$$x(s,t) = \begin{cases} 0, c(s,t) = 0 \\ 1, c(s,t) > 0 \end{cases} \quad (2)$$

$$y(s,t) = \begin{cases} NA, c(s,t) = 0 \\ c(s,t), c(s,t) > 0 \end{cases} \quad (3)$$

The NA indicates that $y(s,t)$ is a random variable that can only take non-zero values, and is therefore undefined when $c(s,t) = 0$. The variable $x(s,t)$ has a Bernoulli distribution, $x(s,t) \sim \text{Bern}(p(s,t))$, while a gamma distribution is used for the $y(s,t)$, $y(s,t) \sim \text{gamma}(a(s,t), b(s,t))$, which has mean $\mu(s,t) = a(s,t)/b(s,t)$. Only the gamma mean is allowed to vary: the variance, $\sigma_g^2 = a(s,t)/b^2(s,t)$, is assumed invariant over space and time.

Next let the $\varepsilon(s,t)$ be a Gaussian Field which is shared by both component random variables in the following way:

$$u(s,t) = \text{logit}(p(s,t)) = \beta_x + \varepsilon(s,t) \quad (4)$$

$$v(s,t) = \log(\mu(s,t)) = \beta_y + \beta_\varepsilon \varepsilon(s,t) \quad (5)$$

where β_x and β_y are intercept parameters (which could be generalized to a covariate model) and the parameter β_ε is a scaling parameter on the shared random effect. Temporal dependence is

introduced through a simple autoregressive model of order 1 (AR(1)), as described in Cameletti et al. (2013), as follows,

$$\varepsilon(s, t) = \rho\varepsilon(s, t-1) + \eta(s, t) \quad (6)$$

where ρ denotes the temporal correlation parameter and $|\rho| < 1$. For a given year, t, the spatial random field (SRF), $\eta(s, t)$, is assumed to be a Gaussian field with mean zero and covariance matrix Σ. We assume a stationary Matérn model (Cressie, 1993) for the spatial covariance model, which specifies how the dependence between observations at two locations decreases with increasing distance. Models were fitted in R using the R-INLA package (Lindgren & Rue, 2015), which uses a computationally efficient Bayesian approach to fitting spatial and spatio-temporal models. Further details are available in Webster et al. (2020).

RESULTS

Pacific halibut larvae were found during the NOAA ichthyoplankton survey in 2005 east of Kodiak Island, but there was no sampling at those stations in 2009 (Figure 3). Larvae were found in both study years in and around Unimak Pass, and in Bering Canyon. In 2005, larvae were present on the north side of the Alaska Peninsula in the BS and over Bering Canyon, but in 2009, larvae were absent along the north side of the Alaska Peninsula east of the 200 m isobath. Pacific halibut larvae were not found after May in either year. Empirical larval distributions from the supplemental study years were similar to the two focus years (Supplemental Figure 1; Supplemental Table 1).

When comparing larval characteristics of the two primary study years, the month of May was selected because of similar sampling coverage between the two years, and the assumption that spawn timing did not differ substantially between years such that larvae that were present in the water column during a particular month were roughly the same age between years. The catch weighted mean length in 2009 (15.38 mm ± 5.03) was ~87% that of 2005 (17.62 mm ± 6.79) for both the BS and GOA combined, and the average standardized catch of larvae/10 m^2 in 2009 (0.4 larvae/10m^2 ± 2.1) was only 20% that of the 2005 catch (2.0 larvae/10m^2 ± 6.6) (Table 2). When those two annual cohorts were sampled two years later during the NOAA groundfish trawl surveys, the estimated abundance of the 2005 year class was ~53% higher than that of the 2009

year class for the BS and GOA combined, but the average fork length was significantly less for the 2005 cohort than for 2009 both in the GOA and BS (*t*-test *p*-value-0.0027).

Larval dispersal pathways

IBM results from focal study years, 2005 and 2009, and representative spawn locations throughout the GOA and BS showed that, generally, larvae were advected westward away from the spawning subregions in the GOA, and were transported northwest in the BS along the continental slope (ex: 200 m isobath; Figs. 1, 4-6). Larvae spawned in the BS (Spawn Region 1, Figure 2) remained north of the Aleutian Islands throughout their pelagic larval stage (Figure 4) and were transported along the continental slope to arrive at the Pacific coast of Asia within ~3 months. Within 6 months post-release, simulated larvae had the potential for widespread dispersal along the Asiatic coastline and north through the Bering Strait in both the focal and supplemental modeled years (Figure 4; Supplemental Figure 2). In 2005 (Figure 4a), larval dispersal to the western BS was greater than in 2009 (Figure 4b). A portion of the larvae that were spawned in the western GOA (Spawn Region 2; Figure 2) arrived to the BS from the GOA within 1-3 months and were primarily transported through island passes, including high larval densities near Unimak Pass, in all study years (Figure 5; Supplemental Figure 3). Transport to the northwest in the BS appeared greater in 2005 (a warm year; Figure 5a) compared with 2009 (a cold year; Figure 5b), especially for larvae that were spawned in the earlier months. Larvae that were not transported to the BS were either retained in the western GOA or advected to the eastern Aleutian Islands. A similar pattern of dispersal to the west and through Aleutian Island passes was observed for Spawn Region 3, but there was higher retention of larvae in the GOA and reductions in dispersal to the BS compared with Spawn Region 2 (Figure 2; Supplemental Figure. 4). Dispersal from the GOA to the BS from the easternmost spawn regions was minimal, but dispersal within the GOA was widespread along the GOA coastline (Spawn Regions 4 and 5; Figures 2 and 6; Supplemental Figures 5 and 6). Larvae that originated from Spawn Region 4 arrived to the BS within 4-5 months, but the majority of larvae were retained in the GOA in the vicinity of Unimak Pass and were not transported westward along the Aleutian Islands (Supplemental Figure 5). The easternmost Spawn Region (Spawn Region 5; Figure 2) showed minimal connectivity between GOA and the BS, with indications that only late stage larvae had the potential to traverse the GOA and arrive in the BS after ~6 month pelagic larval duration

(Figure 6). A large proportion of the larvae from Spawn Region 5 were retained in the eastern GOA and some were transported southward along the coast as well as offshore (Supplemental Figure 6). Connectivity with the western GOA was greatest in the earlier spawn months and there did not appear to be notable differences between the two primary study years of 2005 and 2009 (Figure 6).

Comparisons among warm (2003-2005) and cold (2009-2011) stanza years showed generally consistent sub-regional patterns in connectivity and transport according to the larval transport model (Table 3). Larvae that originated in the BS (Spawn Region 1), remained within the BS ecosystem throughout their trajectories (Supplemental Figure 2). The highest degree of connectivity as well as the greatest interannual variability in connectivity from GOA spawn locations to the BS occurred from Spawn Region 2 where 47-58% of the larvae had the potential to be advected into the BS depending on year (Table 3; Supplemental Figure 3). The majority of simulated larvae from Spawn Region 3 remained in the GOA, but ~15-21% had the potential to be advected into the BS (Table 3; Supplemental Figure 4). This contrasted with Spawn Regions 4 and 5 where very few modeled larvae arrived to the BS (<10% and <2%, respectively; Table 3, Supplemental Figures 5 and 6). From Spawn Region 1, there was potential in every modeled year for arrival to north Pacific Asiatic coastal regions and in some years, the Arctic (Supplemental Figure 2). The model also showed that there was potential for the arrival of larvae to the north Pacific Asiatic coast from Spawn Regions 2 and 3 in some years (Supplemental Figures 3 and 4). Larvae from Spawn Regions 4 and 5 were not likely to reach the north Pacific Asiatic coast, but were dispersed throughout the GOA (Supplemental Figures 5 and 6).

Empirical larval observations and IBM trajectories both show concentrations of larvae around island passes and dispersed through the western GOA and eastern BS along the 200-m isobath (Figures 3-6; Supplemental Figures 1-6). In contrast with empirical larval observations that showed larvae to the east of Unimak Pass in 2005 (Figure 3), almost no IBM trajectories crossed the isobaths along the continental slope to arrive on the continental shelf in the BS (Figures 4-6; Table 3; Supplemental Figures 2-6). In addition, IBM results did not show larval transport to the western Aleutian Islands where there is a known population of Pacific halibut (Seitz et al. 2008). Large-scale qualitative comparisons are possible as described here, but detailed quantitative comparisons between empirical presence and modelled trajectories present challenges due to the limited spatial and temporal scope of larval surveys during each year.

Ontogenetic migration

The spatial model output suggests that as 2 year olds, the 2005 cohort was concentrated in Bristol Bay in the BS and around Kodiak Island in the GOA, and the BS component appears to have stayed aggregated as they began to emerge from Bristol Bay, with distributional centers that moved west and south along the Alaska Peninsula in the immediate subsequent years (Figure 7; Supplemental Figure 7). By age 4, young Pacific halibut were clustered on both sides of Unimak Pass in contrast to younger fish that were concentrated inshore in the southeast BS. Age-5 and age-6 fish appeared less aggregated and were dispersed over a wider range and to deeper depths than younger fish. These patterns in distributional changes over time were generally consistent in other large cohorts from 2003 and 2004 (Supplemental Figures 8 and 9, respectively), with apparent dispersal outwards from inside shallow waters of Bristol Bay and south of Nunivak Island (ages 3-4 years), and subsequent aggregation around Unimak Pass (ages 4-6 years).

Model output suggests that the 2009 cohort was more evenly dispersed overall compared to the 2005 cohort at comparable ages (Figure 8; Supplemental Figure 10), lacking the obvious high-density concentrations of the earlier cohort (note the different scales on the two figures). A primary difference from 2005 was that, in addition to a part of the population leaving Bristol Bay and migrating southward along the Alaska Peninsula as seen with the 2005 cohort, a portion of the 2009 year class also continued to occupy the Bristol Bay area as they aged and were not migrating outward to other parts of the BS to the same degree as the 2005 cohort. There was some indication that there were aggregations around Unimak Pass, but there were no obvious aggregations in the GOA. Overall average abundance (Table 2) and sample sizes (Table 4) were relatively low, making it difficult to observe small scale density changes in this cohort. However, according to the model, distributional changes with age were generally similar for other low-density cohorts from 2010 and 2011 (Supplemental Figures 11 and 12; Supplemental Table 2), although with some differences in timing and dispersal (e.g., the 2010 and 2011 cohorts both showed a stronger clustering south of Nunivak Island in 2015).

DISCUSSION

Developing an understanding of cross-ecosystem population connectivity can inform management strategies for Pacific halibut by providing information about dispersal, migration,

and habitat use across multiple life stages. Model results suggest consistent and substantial larval connectivity between the western GOA and the BS. Pacific halibut larvae that originated in the western GOA have the potential to be transported to the BS, and those larvae that originated from populations in the BS are likely transported northwest along the isobaths in the BS. In addition to larval dispersal, age-specific distributions of Pacific halibut showed ontogenetic range expansions, suggesting that juveniles radiate from their settlement areas in the BS to regions throughout the continental shelf, and potentially reach the Aleutian Islands and the GOA. Spawning in the GOA may provide access to important settlement habitats in the BS, and the potential reverse migration from the BS to the GOA may be important for access to suitable habitats for older life stages, or for maintaining source populations that facilitate access to juvenile settlement habitats.

Biophysical modeling results suggest that the Aleutian Islands constrain larval connectivity between the GOA and the BS, but that island passes are corridors that connect the two ecosystems. Several studies have highlighted oceanographic connectivity between the GOA and the BS through large island passes (Royer, 1981; Reed & Schumacher, 1986; Stabeno et al., 1995) with estimates of ~30% of the Alaska Coastal Current (Aagaard et al., 2006) transported from the GOA to the BS through Unimak Pass (Stabeno et al., 2016a). For pelagic larvae, island passes could facilitate connectivity between the GOA and the BS. IBM results suggest a link between the two basins via large island passes in the eastern Aleutian Islands where an estimated average of 35% of larvae that originated in the western GOA (Spawn Regions 2 and 3) were transported into the BS.

The majority of larval dispersal modeling studies in the North Pacific to date have focused on the GOA or the BS in isolation; however, some studies hypothesize that larvae that were spawned in the western GOA and subsequently exited the study area were potentially transported further west to the Aleutian Islands or into the BS (e.g. Gibson et al., 2019). One study to provide evidence of basin connectivity was that of Parada et al. (2016) that modeled walleye pollock (*Gadus chalcogrammus*) larval transport. Coinciding with our results, several studies have highlighted east-west connectivity in the GOA, particularly between spawning grounds in the eastern GOA and nursery areas in the central GOA for sablefish (*Anoplopoma fimbria*) (Gibson et al., 2019), Pacific cod (*Gadus microcephalus*) (Hinckley et al., 2019), arrowtooth flounder (*Atheresthes stomias*) (Stockhausen et al., 2019a), and Pacific ocean perch (*Sebastes*

alutus) (Stockhausen et al., 2019b). Dispersal patterns in the BS were typically south to north, coinciding with other modeling studies for walleye pollock (Petrik et al. 2016), northern rock sole (Cooper et al. 2013), and Greenland halibut (Duffy-Anderson et al. 2013). Simulated Pacific halibut larvae in the BS were primarily transported along the continental slope, with some larvae reaching the north Pacific Asiatic coastline or transitioning through the Bering Strait.

The prevailing east to west modelled larval transport in the GOA and the south to north trajectories in the BS along the 50-200 m isobaths agree with the prevailing currents in each respective ecosystem (Stabeno et al., 2002; 2004), and with empirical data showing larval concentrations near island passes. However, smaller-scale comparisons with empirical data suggest that model limitations likely impacted finer scale connectivity patterns and transport trajectories. The absence of simulated larval transport to inshore regions of the BS conflicts with the empirical larval distributions during 2005 where larvae were found north of Unimak Pass along the Alaska Peninsula. In addition, according to catch data from the NOAA Fisheries bottom trawl surveys, young demersal stage Pacific halibut are consistently found in high abundance near shore in the southeastern BS. Together, these empirical data suggest that larval transport to the southeastern BS may be much greater than portrayed in the advection modeling. Thus, an understanding of larval access to nurseries is hindered by the probable modeling limitation of under-representing larval transport to inshore habitats in the BS. Another consideration when spatially contemplating nursery occupation, is that demersal-stage juveniles are essentially invisible to survey gear from settlement to 2 years of age and considerable migration may occur during that time. Discrepancies between modeled and empirical abundances of juvenile flatfish in the BS have been observed in the past utilizing an earlier ROMS iteration (Cooper et al., 2013), suggesting that the IBM may be limited in its ability to simulate cross-isobath transport. There are several mechanisms that may impact the ability for the oceanographic model to capture cross-shelf transport. Cross-shelf transport associated with sub-mesoscale eddies or bathymetric steering via seafloor terrain features may play a role in on-shelf movement that can only be captured with higher resolution ocean models (Hermann et al. 2009; Combes et al. 2013; Gibson et al. 2013; Opdal and Vikebø 2016; Vestfals et al. 2014; Mordy et al. 2019). In addition to potential limitations of the physical model, due to lack of empirical data, the IBM did not incorporate orientation to nurseries or directed horizontal swimming behavior that has been observed for some species (Huijbers et al., 2012; Igulu et al., 2013) and has been

hypothesized to be relevant for nursery recruitment of sablefish (Gibson et al., 2019). Larval swimming abilities and vertical movement that were not captured by the model may also facilitate transport to settlement habitats (Cowen and Castro 1994). For example, rock sole larvae in the BS are likely transported from the slope to the shelf through vertical movement of larvae that is synchronized with tidal periodicity (Wilderbuer et al., 2016). Modeling constraints due to resolution as well as biological parameterization also have the potential to impact quantitative estimates of transport and connectivity. Unlike cross-shelf transport in the BS, the model did capture larval transport through Unimak Pass; however, model resolution may impact estimates of transport and potentially underestimate the contribution of smaller island passes (Gibson et al. 2013).

Despite these potential limitations, basin-scale larval connectivity of Pacific halibut between the GOA and the BS was consistent across years and larval transport patterns suggest that spawning within the southern BS may subsidize components of the population to the west. Along the north Pacific Asiatic coast there is an established population of Pacific halibut (Schmidt 1934; Best 1979) but details of size composition, growth, and migration rates are largely unknown. Modeling results suggest populations of Pacific halibut along the north Pacific Asiatic coast may be supported by spawning in the southern BS and that juvenile settlement in the BS may be subsidized by larvae that originate in the western GOA.

Our modeling approaches did not provide evidence of possible factors that contribute to the determination of cohort strength, in this case fluctuations in abundance observed with the strong 2005 and the weak 2009 year classes. The Thompson-Burkenroad debate in the early part of the twentieth century discussed fishery and environmental factors as separate and distinct possible causes of fluctuations in Pacific halibut abundance (Skud 1975), but more recent studies have concluded that both factors can affect fish populations. Pacific halibut spawning biomass declined in the period between 2005 and 2009 (Stewart & Hicks, 2018), but it has been shown that cohort strength does not correlate well with spawning biomass (Clark & Hare, 2002). However, given that Pacific halibut is a fully exploited resource, fishing pressure may play a role in cohort strength and distribution, either through direct removals from the population or in combination with climate-related factors that apply stress to the population (Planque et al. 2010). Likewise, other studies have shown that variation in the distribution of fish species can be driven primarily by climatic factors (e.g. Sunday et al., 2015; McLean et al., 2018). Although this

modeling effort has illustrated that Pacific halibut early life distributions remained relatively constant over two temperature stanzas, the interaction potential among species occupying a particular habitat can change in response to thermal habitat shifts. (Kleisner et al., 2016). In the case of Pacific halibut, variations in temperature could affect predator and prey species proximity, thus altering Pacific halibut abundance through top down (predation mortality) or bottom-up (food availability) processes (Ferreira et al. 2020; Durant et al. 2007). Furthermore, Hunt et al. (2011) and Sigler et al. (2014), among others, showed that climate impacts recently experienced in the BS can affect the total caloric energy contained within the biological system so that changes in lower trophic levels influence upper trophic levels. Shifting productivity of spawning grounds (Somarakis et al., 2019) and spatial shifting of spawning grounds (Kanamori et al., 2019), both related to temperature, could also play a role in total productivity.

Movement patterns of juvenile Pacific halibut have not been well understood, particularly within the BS and between the BS and GOA. While there was extensive historical tagging of Pacific halibut in the BS and GOA (Best, 1977), recovery rates were generally low and only broad-scale movement pathways from the BS to GOA (Webster et al. 2013) and from shallow inshore waters to offshore habitats could be inferred from these data (Skud, 1977). In addition to widespread dispersal to deeper habitats, the results of the spatio-temporal modeling of demersal Pacific halibut illustrate the specific dispersal patterns of young fish from settlement grounds to a major inter-basin connection pathway by age-4-6 years. These results suggest that juvenile and adult migration occurs counter to larval dispersal. Compensatory Pacific halibut migration from settlement grounds in the southeastern BS south and east to the GOA is further supported by genetic studies that have found a lack of genetic differences between Pacific halibut in the eastern BS and GOA (Nielsen et al. 2010; Drinan et al. 2016). While there were similarities between year classes in their general direction of movement, there were also notable differences. In this study, the weaker 2009 year class occupied similar post-settlement redistribution pathways to the stronger 2005 year class, but appeared less aggregated overall and continued to occupy settlement grounds in Bristol Bay, whereas the 2005 cohort appeared to be highly aggregated as young fish and migrated away from settlement grounds before becoming more widely dispersed at older ages. Modeling of the supplemental years reinforced these inter-annual differences, but the general pattern of distribution was consistent across years and temperature stanzas. It is possible that these pattern differences were in part a response to density-dependent

processes within the nursery areas (Le Pape & Bonhommeau, 2015) that were not investigated here.

We have used the spatiotemporal modelling to infer patterns of movement for individual Pacific halibut cohorts, but factors other than migration can influence the apparent distribution of fish, including factors affecting gear selectivity. The NOAA summer bottom trawl survey does not sample the shallowest waters in the BS inside Bristol Bay, and thus young Pacific halibut in such inshore habitats will be missed by the survey. Indeed, this appears to be what happened to the 2011 cohort, which had no age-2 fish captured in 2013, yet the cohort showed up strongly in Bristol Bay the following year (Supplemental Table 2; Supplemental Figure 12). Selectivity to the trawl gear may also be influenced by habitat type, environmental conditions, or sea state, as documented for some other species (e.g., Somerton et al., 2013; Cooper and Nichol, 2016; and Somerton et al, 2018). While acknowledging that such factors may have some effect on the data and thus our model output, the distributional changes we see are both broad-scale and generally consistent among cohorts. This leads us to conclude that movement of Pacific halibut cohorts over time is the most plausible explanation for the patterns described in our work.

This study contributes new knowledge regarding the life cycle of Pacific halibut in the GOA and BS and is a step towards better understanding stock structure. Connectivity driven by dispersal at the larval stage and migration during the early demersal stage impacts species distributions, and leads to large-scale ecosystem connectivity and habitat use. Basin-wide connectivity and habitat use or dependence among life stages suggests that it is imperative for managers to be aware of potential environmental impacts to various geographic components of the stock. The Pacific halibut fishery is currently managed via an ensemble of stock assessment models that lead to a decision table which outlines risks of various harvest scenarios (Stewart et al. 2020). A better understanding of risk to the spawning biomass and thus the future population as shown here, can lead to improved comprehension of consequences associated with different harvest levels, and provide a connection to how management decisions affecting fish stocks made in one area or region may impact fisheries in other areas, including between ocean basins.

Until recently, details of Pacific halibut early life history dispersal and migration have remained elusive. However, improved data streams and modelling approaches used in this study have supported the notion of broad scale connectivity, as hypothesized in earlier literature. Our building knowledge of Pacific halibut early life history will benefit from future research aimed at

improving our understanding of the relative contributions from geographically distinct spawning grounds to nursery habitats, i.e. the sources of replenishment, as well as of the capabilities of young Pacific halibut to actively migrate prior to their detection in standardized surveys as 2-3 year olds.

AUTHOR CONTRIBUTIONS

JTD, JVP, LLS, and EDG conceptualized the project, formulated the objectives, and planned the research. JTD, LLS, and RAW curated the empirical data, and LLS and RAW analyzed the empirical data. EDG, WTS, and RAW designed the models, and EDG and RAW performed the model simulations, analyzed the model data, and provided the model output figures. EDG, RAW, JTD, LLS, and JVP contributed to the interpretation of results. LLS took the lead in writing the manuscript. All authors contributed to the writing, review and editing of the manuscript, provided critical feedback, and helped shape the final product.

REFERENCES

Aagaard, K., Weingartner, T. J., Danielson, S. L., Woodgate, R. A., Johnson, G. C., & Whitledge, T. E. (2006). Some controls on flow and salinity in Bering Strait. Geophys. Res. Ltrs., 33(19). doi:10.1029/2006GL026612

Atwood, E., Duffy-Anderson, J. T., Horne, J. K., & Ladd, C. (2010). Influence of mesoscale eddies on ichthyoplankton assemblages in the Gulf of Alaska. Fish. Oceanogr., 19:493-507. doi:10.1111/j.1365-2419.2010.00559.x

Bailey, K. M., Nakata, H., Van der Veer, H. W. (2005). The planktonic stages of flatfishes: physical and biological interactions in transport processes. Flatfishes: Biology & exploitation: 94-119.

Bailey, K. M., & Picquelle, S. J. (2002). Larval distribution of offshore spawning flatfish in the Gulf of Alaska: potential transport pathways and enhanced onshore transport during ENSO events. Mar. Ecol. Prog. Ser., 236:205-217. doi:10.3354/meps2362015

601 Best, E. (1977). Distribution and abundance of juvenile halibut in the southeastern Bering Sea.
602 Int. Pac. Hal. Comm. Sci. Rep. 62. 23 p.

603 Best, E. (1979). Halibut ecology. [In] Fisheries oceanography – eastern Bering Sea shelf.
604 NWAFC Processed Report 79-20, National Marine Fisheries Service. p. 127-165.

605 Best, E. A. & Hardman, W. H. (1982). Juvenile halibut surveys 1973-1980. Int. Pac. Hal. Comm.
606 Tech. Rep. 20. 38 p.

607 Boeing, W. J. & Duffy-Anderson, J. T. (2008). Ichthyoplankton dynamics and biodiversity in
608 the Gulf of Alaska: responses to environmental change. Ecol. Indicators, 8:292-302.
609 doi:10.1016/j.ecolind.2007.03.002

610 Cameletti, M., Lindgren, F., Simpson, D. & Rue, H. (2013). Spatio-temporal modeling of
611 particulate matter concentration through the SPDE approach. Adv. Stat. Anal. 97:109–
612 131. doi:10.1007/s10182-012-0196-3.

613 Cavole, L. M., Demko, A. M., Diner, R. E., Giddings, A., Koester, I., Pagniello, C. M. L. S.,
614 Paulsen, M-L, Ramiriz-Valdez, A., Schwenck, S. M., Yen, N. K., Zill, M. E., & Franks,
615 P. J. S. (2016). Biological impacts of the 2013-2015 warm-water anomaly in the
616 northeast Pacific: Winners, losers, and the future. Oceanography, 29:273-285.

617 Clark, W. G. & Hare, S. R. (1998). Accounting for bycatch in management of the Pacific halibut
618 fishery. N. American J. Fish. Manag. 18:809-821. doi:10.1577/1548-
619 8675(1998)018<0809:AFBIMO>2.0.CO;2

620 Clark, W. G. & Hare, S. R. (2002). Effects of climate and stock size on recruitment and growth
621 of Pacific halibut. N. Amer. J. Fish. Manag. 22:852-862. doi:10.1577/1548-
622 8675(2002)022<0852:EOCASS>2.0.CO;2

623 Clark, W. G., St-Pierre, G., & Brown, E. S. (1997). Estimates of halibut abundance from NMFS
624 trawl surveys. Int. Pac. Halibut Comm. Tech. Rep. 37. 51 p.

Combes, V., Chenillat, F., Di Lorenzo, E., Rivière, P., Ohman, M. D., & Bograd, S. J. (2013). Cross-shore transport variability in the California Current: Ekman upwelling vs. eddy dynamics. Progress in Oceanography 109: 78–89. doi:10.1016/j.pocean.2012.10.001

Cooper, D. W., Duffy-Anderson, J. T., Stockhausen, W. T., & Cheng, W. (2013). Modeled connectivity between northern rock sole (*Leipdopsetta polyxystra*) spawning and nursery areas in the eastern Bering Sea. J. Sea Res., 84, 2-12. doi:10.1016/j.seares.2012.07.001

Cooper, D. W., & Nichol, D. G. (2016). Juvenile northern rock sole (*Lepidopsetta polyxystra*) spatial distribution and abundance patterns in the eastern Bering Sea: spatially dependent production linked to temperature. ICES Journal of Marine Science, 73(4), 1138–1146. doi:10.1093/icesjms/fsw005

Cowen, R. K., & Castro, L. R. (1994). Relation of coral reef fish larval distributions to island scale circulation around Barbados, West Indies. Bulletin of Marine Science 54: 228–244.

Cressie, N. (1993). Statistics for Spatial Data (2nd ed). Wiley, New York, USA. 928 p.

Danielson, S., Curchitser, E., Hedstrom, K., Weingartner, T., & Stabeno, P. (2011). On ocean and sea ice modes of variability in the Bering Sea. J. Geophys. Res., 116(C12). doi:10.1029/2011JC007389

Drinan, D. P., Galindo, H. M., Loher, T., & Hauser, L. (2016). Subtle genetic population structure in Pacific halibut *Hippoglossus stenolepis*, J. Fish. Bio., 89, 2571-2594. doi: 10.1111/jfb.13148

Dunlop, H. A., Bell, F. H., Myhre, R. J., Hardman, W. H., & Southward, G. M. (1964). Investigation, utilization and regulation of the halibut in southeastern Bering Sea. Int. Pac. Hal. Comm. Rep. 35. 72 p.

Duffy-Anderson, J. T., Blood, D. M., Cheng, W., Ciannelli, L., Matarese, A. C., Sohn, D., Vance, T. C., & Vestfals, C. (2013). Combining field observations and modeling approaches to examine Greenland halibut (Reinhardtius hippoglossoides) early life ecology in the southeastern Bering Sea. J. Sea Res., 75, 96-109. doi:10.1016/j.seares.2012.06.014

652 Duffy-Anderson, J. T., Stabeno, P. J., Siddon, E. C., Andrews, A. G., Cooper, D. W., Eisner, L.
653 B., Farley, E. V., Harpold, C. E., Heintz, R. A., Kimmel, D. G., Sewall, F. F., Spear, A.
654 H., & Yasumishii, E. C. (2017). Return of warm conditions in the southeastern Bering
655 Sea: Phytoplankton – Fish. PLoS ONE, 12, e0178955. doi:10.1371/journal.pone.0178955

656 Duffy-Anderson, J. T., Stabeno, P., Andrews III, A. G., Cieciel, K., Deary, A., Farley, E.,
657 Fugate, C., Harpold, C., Heintz, R., Kimmel, D., Kuletz, K., Lamb, J., Paquin, M., Porter,
658 S., Rogers, L., Spear, A., & Yasumiishi, E. (2019). Responses of the Northern Bering Sea
659 and Southeastern Bering Sea pelagic ecosystems following record-breaking low winter
660 sea ice. Geophys. Res. Lett., 46, 9833-9842. doi:10.1029/2019GL083396

661 Durant, J. M. Hjermann, D. Ø., Ottersen, G., Stenseth, N. C. 2007. Climate and the match or
662 mismatch between predator requirements and resource availability. Clim. Res., 33: 271-
663 283. doi:10.3354/cr033271

664 Ferreira, A. S. A., Stige, L. C., Neuheimer, A. B., Bogstad, B., Yaragma, N., Prokopchuk, I.,
665 Durant, J. M. (2020). Match-mismatch dynamics in the Norwegian Barents Sea system.
666 Mar. Ecol. Prog. Ser. LFCav5. doi:10.3354/meps13276.

667 Forsberg, J. E. (2001). Aging manual for Pacific halibut: procedures and methods used at the
668 International Pacific Halibut Commission. Int. Pac. Halibut Comm. Tech. Rep. 46. 56 p.

669 Gibson, G. A., Coyle, K. O., Hedstrom, K., and Curchitser, E. N. (2013). A modeling study to
670 explore on-shelf transport of oceanic zooplankton in the Eastern Bering Sea. Journal of
671 Marine Systems 121–122: 47–64. doi:10.1016/j.jmarsys.2013.03.010

672 Gibson, G. A., Stockhausen, W. T., Coyle, K. O., Hinckley, S., Parada, C., Hermann, A. J.,
673 Doyle, M., & Ladd, C. (2019). An individual-based model for sablefish: Exploring the
674 connectivity between potential spawning and nursery grounds in the Gulf of Alaska.
675 Deep-Sea Res. Part II, 165, 89-112. doi:10.1016/jdsr2.2018.05.015

676 Goldstein, E. D., Pirtle, J. L., Duffy-Anderson, J. T., Stockhausen, W. T., Zimmermann, M.,
677 Wilson, M. T. and Mordy, C. W. (2020). Eddy retention and seafloor terrain facilitate

cross-shelf transport and delivery of fish larvae to suitable nursery habitats. Limnol Oceanogr. doi:10.1002/lno.11553

Haidvogel, D. B., Arango, H., Budgell, W. P., Cornuelle, B. D., Curchitser, E., DiLorenzo, E., Fennel, K., Geyer, W. R., Hermann, A. J., Lanerolle, L., Levin, J., McWilliams, J. C., Miller, A. J., Moore, M., Powell, T. M., Shchepetkin, A. F., Sherwood, C. R., Signell, R. P., Warner, J. C., & Wilkin, J. (2008). Ocean forecasting in terrain-following coordinates: Formulation and skill assessment of the Regional Ocean Modeling System. J. Comp. Phys., 227, 3595-3624. doi:10.1016/j.jcp.2007.06.016

Hermann, A. J., Gibson, G. A., Bond, N. A., Curchitser, E. N., Hedstrom, K., Cheng, W., Wang, M., Stabeno, P. J., Eisner, L., & Cieciel, K. D. (2013). A multivariate analysis of observed and modeled biophysical variability on the Bering Sea shelf: Multidecadal hindcasts (1970-2009) and forecasts (2010-2040). Deep-Sea Res. II: Top. Stud. Oceanogr., 94, 121-139. doi:10.1016/j.dsr2.2013.04.007

Hermann, A. J., Hinckley, S., Dobbins, E. L., Haidvogel, D. B., Bond, N. A., Mordy, C., Kachel, N., & Stabeno, P. J. (2009). Quantifying cross-shelf and vertical nutrient flux in the Coastal Gulf of Alaska with a spatially nested, coupled biophysical model. Deep Sea Research Part II: Topical Studies in Oceanography **56**: 2474–2486. doi:10.1016/j.dsr2.2009.02.008

Hinckley, S., Stockhausen, W. T., Coyle, K. O., Larel, G. J., Gibson, G. A., Parada, C., Hermann, A. J., Doyle, M. J., Hurst, T. P., Punt, A. E., & Ladd, C. (2019). Connectivity between spawning and nursery areas for Pacific cod (*Gadus microcephalus*) in the Gulf of Alaska. Deep-Sea Res. II., 165, 113-126. doi:10.1016/j.dsr2.2019.05.007

Huijbers, C. M., Nagelkerken, I., Lössbroek, P. A. C., Schulten, I. E., Siegenthaler, A., Holderied, M. W., & Simpson, S. D. (2012). A test of the senses: Fish select novel habitats by responding to multiple cues. Ecol., 93, 46-55. doi:10.1890/10-2236.1

Hunt Jr., G. L., Coyle, K. O., Eisner, L. B., Farley, E. V., Heintz, R. A., Mueter, F., Napp, J. M., Overland, J. E., Ressler, P. H., Salo, S., & Stabeno, P. J. (2011). Climate impacts on eastern Bering Sea foodwebs: a synthesis of new data and an assessment of the

706 Oscillating Control Hypothesis. ICES J. Mar. Sci., 68, 1230-1243.
707 doi:10.1093/icesjms/fsr036

708 Igulu, M. M., Nagelkerken, I., van der Beek, M., Schippers, M., van Eck, R., & Mgaya, Y. D.
709 (2013). Orientation from open water to settlement habitats by coral reef fish: behavioral
710 flexibility in the use of multiple reliable cues. Mar. Ecol. Prog. Ser., 492, 243-257.
711 doi:10.3354/meps10542

712 Kanamori, Y., Takasuka, A., Nishijima, S., & Okamura, H. (2019). Climate change shifts the
713 spawning ground northward and extends the spawning period of chub mackerel in the
714 western North Pacific. Mar. Ecol. Prog. Ser., 624, 155-166. doi:10.3354/meps13037

715 Kimmel, D. G., Eisner, L. B., Wilson, M. T., & Duffy-Anderson, J. T. (2018). Copepod
716 dynamics across warm and cold periods in the eastern Bering Sea: Implications for
717 walleye Pollock (*Gadus chalcogrammus*) and the Oscillating Control Hypothesis. Fish.
718 Oceanogr., 27, 143-158. doi:10.1111/fog.12241

719 Kleisner, K. M., Fogarty, M. J., McGee, S., Barnett, A., Fratantoni, P., Greene, J., Hare, J. A.,
720 Lucey, S. M., McGuire, C., Odell, J., Saba, V. S., Smith, L., Weaver, K. J., & Pinsky, M.
721 L. (2016). The effects of sub-regional climate velocity on the distribution and spatial
722 extent of marine species assemblages. PLoS ONE, 11, e0149220.
723 doi:10.1371/journal.pone.0149220

724 Le Pape, O., & Bonhommeau, S. (2015). The food limitation hypothesis or juvenile marine fish.
725 Fish and Fisheries, 16, 373-398. doi:10.1111/faf.12063

726 Lindgren, F. & Rue, H. (2015). Bayesian spatial modelling with R-INLA. J. Stat. Soft., 63, 1–27.

727 McLean, M., Mouillot, D., Lindegren, M., Engelhard, G., Villeger, S., Marchal, P.,
728 Brind'Amour, A., & Auber, A. (2018). A climate-driven functional inversion of
729 connected marine ecosystems. Curr. Biol., 28, 3654-3660. doi:10.1016/j.cub.2018.09.050

730 Mordy, C. W., Stabeno, P. J, Kachel, N. B., Ladd, C., Zimmermann, M., Hermann, A. J., Coyle,
731 K. O., & Doyle, M. J. (2019). Patterns of flow in the canyons of the northern Gulf of

Alaska. Deep Sea Research Part II: Topical Studies in Oceanography S0967064519301079. doi:10.1016/j.dsr2.2019.03.009

Mumby, P. J., Edwards, A. J., Arias-González, J. E., Lindeman, K. C., Blackwell, P. G., Gall, A., Gorczynska, M. I., Harborne, A. R., Pescod, C. L., Renken, H., Wabnitz, C. C., & Llewellyn, G. (2004). Mangroves enhance the biomass of coral reef fish communities in the Caribbean. Nature, 427, 533-536. doi:10.1038/nature02286

Napp, J. M., Kendall, A. W., & Schumacher, J. D. (2000). A synthesis of biological and physical processes affecting the feeding environment of larval walleye pollock (*Theragra chalcogramma*) in the eastern Bering Sea. Fish. Oceanogr., 9, 147-162.

National Oceanic and Atmospheric Administration (NOAA). (2019). Ichthyoplankton Information System Database, https://access.afsc.noaa.gov/ichthyo/

National Oceanic and Atmospheric Administration (NOAA). (2020). Alaska Groundfish Bottom Trawl Survey Data, https://www.fisheries.noaa.gov/alaska/commercial-fishing/alaska-groundfish-bottom-trawl-survey-data

Nielsen, J. L., Graziano, S. L., & Seitz, A. C. (2010). Fine-scale population genetic structure in Alaskan Pacific halibut (*Hippoglossus stenolepis*). Conserv. Genet., 11, 999-1012. doi:10.1007/s10592-009-9943-8

Norcross, B. L., Muter, F. J., & Holladay, B. A. (1997). Habitat models for juvenile pleuronectids around Kodiak Is., Alaska. Ocean. Lit. Rev. No. 44, 1548.

Norcross, B. L., Blanchard, A., & Holladay, B. A. (1999). Comparison of models for defining nearshore flatfish nursery areas in Alaskan waters. Fish. Oceanogr., 8, 50-67.

Opdal, A. F. & Vikebø, F. B. (2016). Long term stability in modelled zooplankton influx could uphold major fish spawning grounds on the Norwegian continental shelf. Can. J. Fish. Aquat. Sci. 73: 186-196. doi: 10.1139/cjfas-2014-0524

Parada, C., Hinckley, S., Horne, J., Mazur, M., Hermann, A., & Curchister, E. (2016). Modeling connectivity of walleye Pollock in the Gulf of Alaska: Are there any linkages to the

Bering Sea and Aleutian Islands? Deep-Sea Res. II: Top. Stud. Oceanogr., 132, 227-239. doi:10.1016/j.dsr2.2015.12.010

Petitgas, P., Rijnsdorp, A. D., Dickey-Collas, M., Engelhard, G. H., Peck, M. A., Pinnegar, J. K., Drinkwater, K., Huret, M., & Nash, R. D. M. (2013). Impacts of climate change on the complex life cycles of fish. Fish. Oceanogr., 22, 121-139. doi:10.1111/fog.12010

Petrik, C. M., J. T. Duffy-Anderson, F. Castruccio, E. N. Curchitser, S. L. Danielson, K. Hedstrom, and F. Mueter. (2016). Modelled connectivity between Walleye Pollock (Gadus chalcogrammus) spawning and age-0 nursery areas in warm and cold years with implications for juvenile survival. ICES J. Mar. Sci. **73**: 1890–1900. doi:10.1093/icesjms/fsw004

Planque, B., Fromentin, J. M., Cury, P., Drinkwater, K. F., Jennings, S., Perry, R. I., & Kifani, S. (2010). How does fishing alter marine populations and ecosystems sensitivity to climate?. Journal of Marine Systems, 79(3-4), 403-417.

Posgay, J.A. & Marak, R. R. (1980). The MARMAP Bongo Zooplankton Samplers. J. Northw. Atl. Fish. Sci., 1, 91-99.

Reed, R. K. & Schumacher, J. D. (1986). Physical oceanography, [*In*] The Gulf of Alaska. Physical environment and biological resources. Hood, D.W., and Zimmeran, S.T. [*eds*]. U.S. Dept. Comm./NTIS part 2, 57-75.

Rochette, S., Rovot, E., Morin, J., Mackinson, S., Riou, P., & Le Pape, O. (2010). Effect of nursery habitat degradation on flatfish population: Application of Solea solea in the eastern channel (Western Europe). J. Sea Res., 64, 34-44. doi:10.1016/j.seares.2009.08.003

Royer, T. C. (1981). Baroclinic transport in the Gulf of Alaska. Part II. A freshwater driven coastal current. J. Mar. Res., 39, 251-265.

Schmidt, P. J. 1934. On the zoogeographical distribution of the chief marine food fishes in the western part of the Pacific. Pacific Science Congress, 5th, Victoria and Vancouver, B. C. 1933. Proceedings v. 5, p. 3796-3797. Toronto, University Press.

785 Seitz, A. C., Loher, T., & Nielsen, J. L. (2008). Seasonal movements and environmental
786 conditions experienced by Pacific halibut along the Aleutian Islands, examined by pop-up
787 satellite tags. Int. Pac. Halibut Comm. Sci. Rep. 85. 24 p.

788 Seitz, A. C., Loher, T., Norcross, B. L., & Nielsen, J. L. (2011). Dispersal and behavior of
789 Pacific halibut *Hippoglossus stenolepis* in the Bering Sea and Aleutian Islands region.
790 Aquat. Biol., 12, 225-239. doi:10.3354/ab00333

791 Shchepetkin, A. F. & McWilliams, J. C. (2005). The regional oceanic modeling system (ROMS):
792 a split-explicit, free surface, topography-following-coordinate oceanic model. Ocean
793 Model., 9, 347-404. doi:10.1016/j.ocemod.2004.08.002

794 Sigler, M. F., Stabeno, P. J., Eisner, L. B., Napp, J. M., & Mueter, F. J. (2014). Spring and fall
795 phytoplankton blooms in a productive subarctic ecosystem, the eastern Bering Sea,
796 during 1995-2011. Deep-Sea Res. Part II, 109, 71-83. doi:10.1016/j.dsr2.2013.12.007

797 Skud, B. E. (1975). Revised estimates of halibut abundance and the Thompson-Burkenroad
798 debate. Int. Pac. Halibut Comm. Sci. Rep. 56. 36 p.

799 Skud, B. E. (1977). Drift, migration, and intermingling of Pacific halibut stocks. Int. Pac. Halibut
800 Comm. Sci. Rep. 63. 42 p.

801 Smith, P. E., & Richardson, S. R. (1977). Standard techniques for pelagic fish egg and larva
802 surveys. FAO Fish. Tech. Pap., No. 175. 100 p.

803 Sohn, D. (2016). Distribution, abundance, and settlement of slope-spawning flatfish during early
804 life stages in the eastern Bering Sea. PhD Dissertation. Oregon State University,
805 Corvallis, OR, U.S.A.

806 Sohn, D., Ciannelli, L., & Duffy-Anderson, J. T. (2016). Distribution of early life Pacific halibut
807 and comparison with Greenland halibut in the eastern Bering Sea. J. Sea Res., 107, 31-42.
808 doi:10.1016/j.seares.2015.09.001

809 Somarakis, S., Tsoukali, S., Giannoulaki, M., Schismenou, E., & Nikolioudakis, N. (2019).
810 Spawning stock, egg production and larval survival in relation to small pelagic fish
811 recruitment. Mar. Ecol. Prog. Ser., 617-618, 113-136. doi:10.3354/meps12642

812 Somerton, D. A., Weinberg, K. L., & Goodman, S. E. (2013). Catchability of snow crab
813 (*Chionoecetes opilio*) by the eastern Bering Sea bottom trawl survey estimated using a
814 catch comparison experiment. Can. J. Fish. Aquat. Sci. 70: 1699–1708
815 dx.doi.org/10.1139/cjfas-2013-0100

816 Somerton, D., Weinberg, K., Munro, P., Rugolo, L., & Wilderbuer, T. (2018). The effects of
817 wave-induced vessel motion on the geometry of a bottom survey trawl and the herding of
818 yellowfin sole (*Limanda aspera*). Fish. Bull. 116:21–33. doi: 10.7755/FB.116.1.3

819 Spies, I. (2012). Landscape genetics reveals population subdivision in Bering Sea and Aleutian
820 Islands Pacific cod. Trans. Am. Fish. Soc., 141(6), 1557-1573.
821 doi:10.1080/00028487.2012.711265

822 St. Pierre, G. (1989). Recent studies of Pacific halibut postlarvae in the Gulf of Alaska and
823 eastern Bering Sea. Int. Pac. Halibut Comm. Sci. Rep. 73. 31 p.

824 St. Pierre, G. (1984). Spawning locations and season for Pacific halibut. Int. Pac. Halibut Comm.
825 Sci. Rep. 70. 46 p.

826 Stabeno, P. J., Reed, R. K., & Schumacher, J. D. (1995). The Alaska Coastal Current: continuity
827 of transport and forcing. J. Geo. Res.: Oceans, 100, 2477-2485. doi:10.1029/94JC02842

828 Stabeno, P. J., Schumacher, J. D., & Ohtani, K. (1999). Chapter 1: The physical oceanography of
829 the Bering Sea. [*In*] Dynamics of the Bering Sea. Loughlin, T. R. & Ohtani, K. [*eds.*]
830 Alaska Sea Grant, University of Alaska, Fairbanks.

831 Stabeno, P. J., Reed, R. K., & Napp, J. M. (2002). Transport through Unimak Pass, Alaska.
832 Deep-Sea Res. II, 49, 5919-5930. doi:10.1016/S0967-0645(02)00326-0

833 Stabeno, P. J., Bond, N. A., Hermann, A. J., Kachel, N. B., Mordy, C. W., & Overland, J. E.
834 (2004). Meteorology and oceanography of the Northern Gulf of Alaska. Cont. Shelf Res.,
835 24, 859-897. doi:10.1016/j.csr.2004.02.007

836 Stabeno, P. J., Kachel, N. B., Moore, S. E., Napp, J. M., Sigler, M. Yamaguchi, A., & Zerbini, A.
837 N. (2012). Comparison of warm and cold years on the southeastern Bering Sea shelf and
838 some implications for the ecosystem. Deep-Sea Res. II, 65-70, 31-45.
839 doi:10.1016/j.dsr2.2012.02.020

840 Stabeno, P. J., Bell, S., Cheng, W., Danielson, S., Kachel, N. B., & Mordy, C. W. (2016a). Long-
841 term observations of Alaska Coastal Current in the northern Gulf of Alaska. Deep-Sea
842 Res. II, 132, 24-40. doi:10.1016/j.dsr2.2015.12.016

843 Stabeno, P. J., Danielson, S. L., Kachel, D. G., Kachel, M. B., & Mordy, C. W. (2016b).
844 Currents and transport on the Eastern Bering Sea shelf: An integration of over 20 years of
845 data. Deep-Sea Res. Part II, 134, 13-29. doi:10.1016/j.dsr2.2016.05.010

846 Stauffer, G. (2004). NOAA protocols for groundfish bottom trawl surveys of the nation's fishery
847 resources. U. S. Dept. Commerce NOAA Tech. Memo. NMFS-F/SPO-65. 205 p.

848 Stewart, I. & Hicks, A. (2018). Assessment of the Pacific halibut (*Hippoglossus stenolepis*) stock
849 at the end of 2018. Int. Pac. Halibut Comm. Annual Meeting Report: IPHC-2019-
850 AM095-09.

851 Stewart, I., Hicks, A., Webster, R., & Wilson, D. (2020) Summary of the data, stock assessment,
852 and harvest decision table for Pacific halibut (*Hippoglossus stenolepis*) at the end of
853 2019. Int. Pac. Halibut Comm. Annual Meeting Report: IPHC-2020-AM096-09 Rev_2.

854 Stockhausen, W. T., Coyle, K. O., Hermann, A. J., Blood, D., Doyle, M. J., Gibson, G. A.,
855 Hinckley, S., Ladd, C., & Parada, C. (2019a). Running the gauntlet: Connectivity
856 between spawning and nursery areas for arrowtooth flounder (*Atheresthes stomias*) in the
857 Gulf of Alaska, as inferred from a biophysical individual-based model. Deep-Sea Res. II,
858 165, 127-139. doi:10.1016/j.dsr2.2018.05.017

Stockhausen, W. T., Coyle, K. O., Hermann, A. J., Doyle, M. J., Gibson, G. A., Hinckley, S., Ladd, C., & Parada, C. (2019b). Running the gauntlet: Connectivity between natal and nursery areas for Pacific ocean perch (*Sebastes alutus*) in the Gulf of Alaska, as inferred from a biophysical individual-based model. Deep-Sea Res. II, 165, 74-88. doi:10.1016/j.dsr2.2018.05.016

Stoner, A. W., & Abookire, A. A. (2002). Sediment preferences and size-specific distribution of young-of-the-year Pacific halibut in an Alaska nursery. Fish. Biol., 61, 540-559. doi:10.1111/j.1095-8649.2002.tb00895.x

Sunday, J. M., Pecl, G. T., Frusher, S., Hobday, A. J., Hill, N., Holbrook, N. J., Edgar, G. J., Stuart-Smith, R., Barrett, N., Wernberg, T., Watson, R. A., Smale, D. A., Fulton, E. A., Slawinski, D., Feng, M., Radford, B. T., Thompson, P. A., & Bates, A. E. (2015). Species traits and climate velocity explain geographic range shifts in an ocean-warming hotspot. Ecol. Lett., 18, 944-953. doi:10.1111/ele.12474

Thompson, W. F. & Van Cleve, R. (1936). Life history of the Pacific halibut. Int. Fish Comm. Rep. 9. 205 p.

Vestfals, C. D., Ciannelli, L., Duffy-Anderson, J. T., & Ladd, C. (2014). Effects of seasonal and interannual variability in along-shelf and cross-shelf transport on groundfish recruitment in the eastern Bering Sea. Deep Sea Research Part II: Topical Studies in Oceanography 109: 190–203. doi:10.1016/j.dsr2.2013.09.026

Webster, R. A., Clark, W. G., Leaman, B. M., & Forsberg, J. E. (2013). Pacific halibut on the move: a renewed understanding of adult migration from a coastwide tagging study. Can. J. Fish. Aquat. Sci., 70, 642-653. doi:10.1139/cjfas-2012-0371

Webster, R. A., Soderlund, E., Dykstra, C. L., & Stewart, I. J. (2020). Monitoring change in a dynamic environment: spatio-temporal modelling of calibrated data from different types of fisheries surveys of Pacific halibut. Can. J. Fish. Aquat. Sci., 77:1421-1432. doi.org/10.1139/cjfas-2019-0240

Wilderbuer, T., Duffy-Anderson, J. T., Stabeno, P., & Hermann, A. (2016). Differential patterns of divergence in ocean drifters: Implications for larval flatfish advection and recruitment. J. Sea Res., 111, 11-24. doi:10.1016/j.seares.2016.03.003

TABLES

TABLE 1 Early life history parameters used for the Pacific halibut larval dispersal individual based biophysical model. The model simulation was terminated once a larva reached the newly-settled juvenile stage after 180 days. Information adapted from Table 3.1 in Sohn (2016)

Developmental stage	Duration (days)	Depth range (m)	Vertical swimming speed (m/s)	Vertical diffusion (m/s)
Eggs	20	400-500	0.00006	0.0001
Yolksac/Preflexion larvae	55	100-400	0.002	0.001
Flexion larvae	45	10-100	0.004	0.001
Postflexion larvae	35	10-100	0.006	0.001
Transformation	25	10-100	0.01	0.001
Newly-settled juveniles	N/A	10-100	0.02	0.001

TABLE 2 Mean catch (number/10m^2) and size (mm) of larval Pacific halibut caught during the NOAA icthyoplankton surveys in May of 2005 and 2009 in the Bering Sea (BS) and Gulf of Alaska (GOA), in addition to estimated abundance (millions of fish) and mean length (cm) of those same year classes when sampled two years later during the NOAA groundfish bottom trawl surveys

Larvae

	Catch-weighted mean length (mm)	Std dev of Catch-weighted mean length	Min size sampled (mm)	Max size sampled (mm)	# measured	Mean catch/10m^2	Std dev of mean catch	# hauls
2005								
BS	17.31	7.23	8.2	21.0	51	2.5	8.0	135
GOA	18.04	6.20	10.0	26.0	38	1.6	5.2	163
Combined	17.62	6.79			89	2.0	6.6	298
2009								
BS	15.18	5.23	9.7	18.6	12	0.7	2.7	92
GOA	19.50	n/a	19.5	19.5	1	< 0.1	0.4	66
Combined	15.38	5.03			13	0.4	2.1	158

2 year old fish

	Estimated abundance (Mfish)	Mean length (cm)	Std dev of mean length	# measured
2005 year class (BS)	31.42	19.4	3.1	227
2005 year class (GOA)	1.84	24.7	3.4	204

2005 combined	33.26	21.9	4.2	
2009 year class (BS)	13.22	21.4	3.4	30
2009 year class (GOA)	2.34	26.4	3.8	26
2009 combined	15.56	23.7	4.3	

TABLE 3 Percentage of Pacific halibut larvae arriving in the Bering Sea (BS), based on a division between the GOA and BS along the Aleutian Island chain, from each of five spawn regions (Figure 2) for each study year estimated by the individual-based biophysical model (IBM).

Spawn region	Year					
	Warm			Cold		
	2003	2004	2005	2009	2010	2011
1	100	100	100	100	100	100
2	58.0	51.1	58.1	52.7	51.5	47.0
3	17.6	19.3	15.2	17.2	17.2	20.5
4	8.6	4.5	8.2	4.5	7.0	6.5
5	0.2	0.04	0.6	0.08	1.6	0.04

TABLE 4 Sample sizes of aged Pacific halibut from NMFS trawl surveys used in the spatio-temporal modelling, by cohort year, body of water, and age (years).

Age	Cohort			
	2005		2009	
	Bering Sea	GOA	Bering Sea	GOA
2	227	204	30	26
3	510		42	
4	590	633	59	56
5	333		66	
6	411	727	25	48

FIGURE LEGENDS

FIGURE 1 Schematic of major ocean circulation patterns in the Gulf of Alaska and Bering Sea. Compiled from information available in Stabeno et al. (1999), Stabeno et al. (2004), and Stabeno et al. (2016b)

FIGURE 2 Five regions (color coded) used to define egg/larva origin points for larval advection modeling. Regions are based on major known spawning locations for Pacific halibut identified in St. Pierre (1984).

FIGURE 3 Catch-per-unit-effort (number/10m^2) of Pacific halibut larvae caught during the NOAA Fisheries EcoFOCI Icthyoplankton surveys in the study years of 2005 (red) and 2009 (blue). Note that sampling occurred in all months February-October in 2005 and those same months excluding August in 2009

FIGURE 4 Maps showing simulated larval densities from the Individual-Based Biophysical Model for the (a) 2005 and (b) 2009 year classes with simulated larval release points from Spawn Region 1 (see Figure 2). For each spawn month (November-March), counts of individual simulated larvae were summed within 0.5^o latitude and longitude grid cells following 1 month (days 0-30), 3 months (days 61-90), and 6 months (days 151-180) post-spawn. The transparency of the color scale reflects larval density in each grid cell and the color shows the time period post-spawning

FIGURE 5 Maps showing simulated larval densities from the Individual-Based Biophysical Model (IBM) for the (a) 2005 and (b) 2009 year classes with simulated larval release points from Spawn Region 2 (see Figure 2). For each spawn month (November-March), counts of individual simulated larvae were summed within 0.5^o latitude and longitude grid cells following 1 month (days 0-30), 3 months (days 61-90), and 6 months (days 151-180) post-spawn. The transparency of the color scale reflects larval density in each grid cell and the color shows the time period post-spawning

FIGURE 6 Maps showing simulated larval densities from the Individual-Based Biophysical Model (IBM) for the (a) 2005 and (b) 2009 year classes with simulated larval release points from Spawn Region 5 (see Figure 2). For each spawn month (November-March), counts of individual simulated larvae were summed within 0.5^o latitude and longitude grid cells following 1 month (days 0-30), 3 months (days 61-90), and 6 months (days 151-180) post-spawn. The transparency

of the color scale reflects larval density in each grid cell and the color shows the time period post-spawning

FIGURE 7 Posterior predictions of catch-per-unit-effort (left) and corresponding posterior standard deviations for 2-6 year old Pacific halibut caught during the NOAA Alaska Fisheries Science Center summer bottom trawl surveys for the 2005 cohort

FIGURE 8 Posterior predictions of catch-per-unit-effort (left) and corresponding posterior standard deviations for 2-6 year old Pacific halibut caught during the NOAA Alaska Fisheries Science Center summer bottom trawl surveys for the 2009 cohort

SUPPORTING INFORMATION

SUPPLEMENTAL TABLE 1. Number of stations sampled during the NOAA Ichthyoplankton surveys for 2003, 2004, 2005, 2009, 2010, and 2011 by month.

SUPPLEMENTAL TABLE 2. Sample sizes of aged Pacific halibut from NMFS trawl surveys used in the spatiotemporal modelling for the 2003, 2004, 2010, and 2011 cohorts.

SUPPLEMENTAL FIGURE 1 Catch-per-unit-effort (number/10m^2) of Pacific halibut larvae caught during the NOAA Fisheries Ichthyoplankton surveys for the study years of 2003-2005 and 2009-2011.

SUPPLEMENTAL FIGURE 2 Maps showing the distributions of simulated larvae from the individual based biophysical model for larvae spawned from Spawn Location 1 (See Figure 2) for the years a) 2003, b) 2004, c) 2005, d) 2009, e) 2010, and f) 2011. Daily larval locations are shown as points and the colors show the simulated larval release month. The panels show a snapshot of the respective year and month in the model simulation (i.e. daily larval locations throughout each observation month are plotted as points).

SUPPLEMENTAL FIGURE 3 Maps showing the distributions of simulated larvae from the individual based biophysical model for larvae spawned from Spawn Location 2 (See Figure 2)

for the years a) 2003, b) 2004, c) 2005, d) 2009, e) 2010, and f) 2011. Daily larval locations are shown as points and the colors show the simulated larval release month. The panels show a snapshot of the respective year and month in the model simulation (i.e. daily larval locations throughout each observation month are plotted as points).

SUPPLEMENTAL FIGURE 4 Maps showing the distributions of simulated larvae from the individual based biophysical model for larvae spawned from Spawn Location 3 (See Figure 2) for the years a) 2003, b) 2004, c) 2005, d) 2009, e) 2010, and f) 2011. Daily larval locations are shown as points and the colors show the simulated larval release month. The panels show a snapshot of the respective year and month in the model simulation (i.e. daily larval locations throughout each observation month are plotted as points).

SUPPLEMENTAL FIGURE 5 Maps showing the distributions of simulated larvae from the individual based biophysical model for larvae spawned from Spawn Location 4 (See Figure 2) for the years a) 2003, b) 2004, c) 2005, d) 2009, e) 2010, and f) 2011. Daily larval locations are shown as points and the colors show the simulated larval release month. The panels show a snapshot of the respective year and month in the model simulation (i.e. daily larval locations throughout each observation month are plotted as points).

SUPPLEMENTAL FIGURE 6 Maps showing the distributions of simulated larvae from the individual based biophysical model for larvae spawned from Spawn Location 5 (See Figure 2) for the years a) 2003, b) 2004, c) 2005, d) 2009, e) 2010, and f) 2011. Daily larval locations are shown as points and the colors show the simulated larval release month. The panels show a snapshot of the respective year and month in the model simulation (i.e. daily larval locations throughout each observation month are plotted as points).

SUPPLEMENTAL FIGURE 7 Posterior predictions of catch-per-unit-effort (left) and corresponding posterior standard deviations for 2-8 year old Pacific halibut caught during the NOAA Alaska Fisheries Science Center summer bottom trawl surveys for the 2005 year class.

SUPPLEMENTAL FIGURE 8 Posterior predictions of catch-per-unit-effort (left) and corresponding posterior standard deviations for 2-8 year old Pacific halibut caught during the NOAA Alaska Fisheries Science Center summer bottom trawl surveys for the 2003 year class.

SUPPLEMENTAL FIGURE 9 Posterior predictions of catch-per-unit-effort (left) and corresponding posterior standard deviations for 2-8 year old Pacific halibut caught during the NOAA Alaska Fisheries Science Center summer bottom trawl surveys for the 2004 year class.

SUPPLEMENTAL FIGURE 10 Posterior predictions of catch-per-unit-effort (left) and corresponding posterior standard deviations for 2-8 year old Pacific halibut caught during the NOAA Alaska Fisheries Science Center summer bottom trawl surveys for the 2009 year class.

SUPPLEMENTAL FIGURE 11 Posterior predictions of catch-per-unit-effort (left) and corresponding posterior standard deviations for 2-8 year old Pacific halibut caught during the NOAA Alaska Fisheries Science Center summer bottom trawl surveys for the 2010 year class.

SUPPLEMENTAL FIGURE 12 Posterior predictions of catch-per-unit-effort (left) and corresponding posterior standard deviations for 3-7 year old Pacific halibut caught during the NOAA Alaska Fisheries Science Center summer bottom trawl surveys for the 2011 year class. Note that there were no 2-year-old fish caught during the Bering Sea survey so we did not model this age class for this cohort.

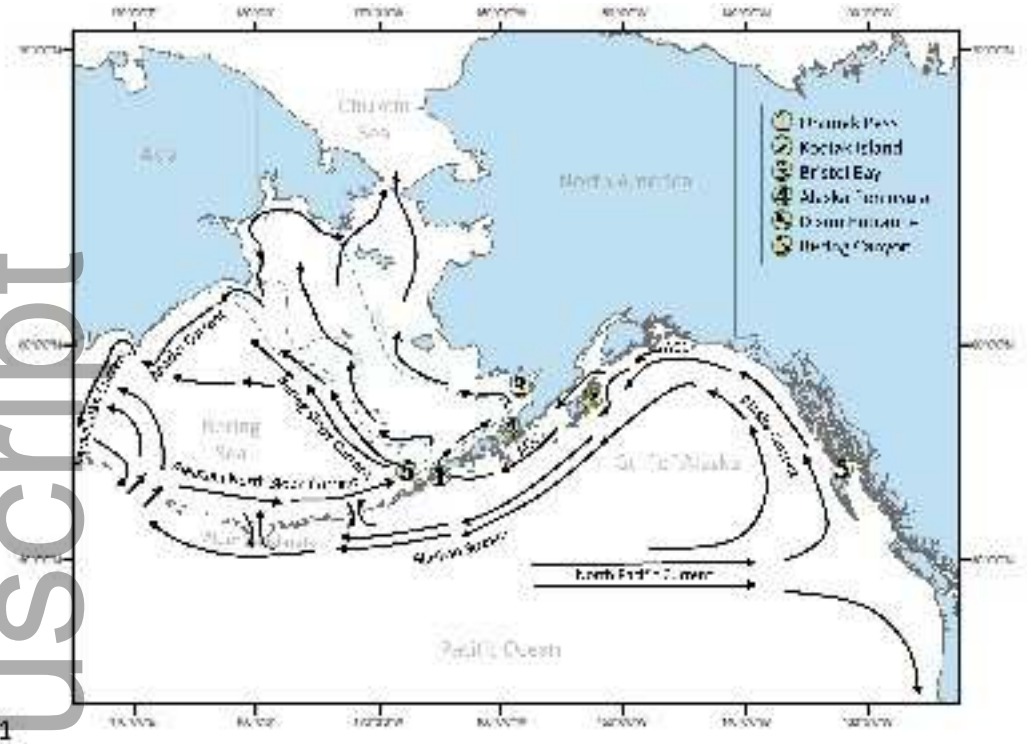

Figure 1

fog_12512_f1.tiff

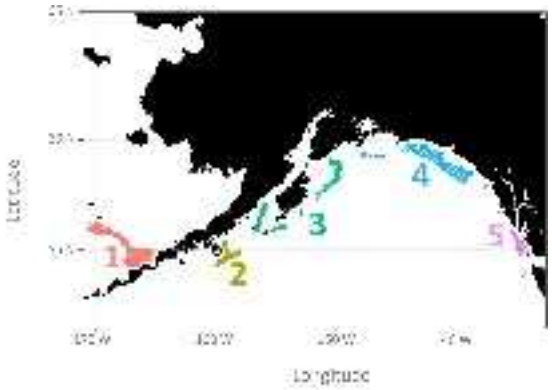

Figure 2

fog_12512_f2.tiff

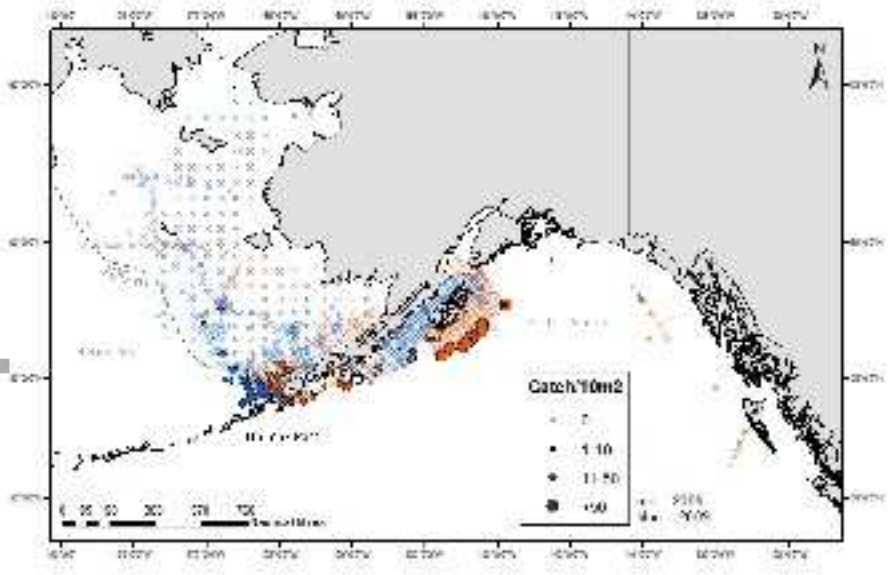

Figure 3

fog_12512_f3.tiff

Figure 4

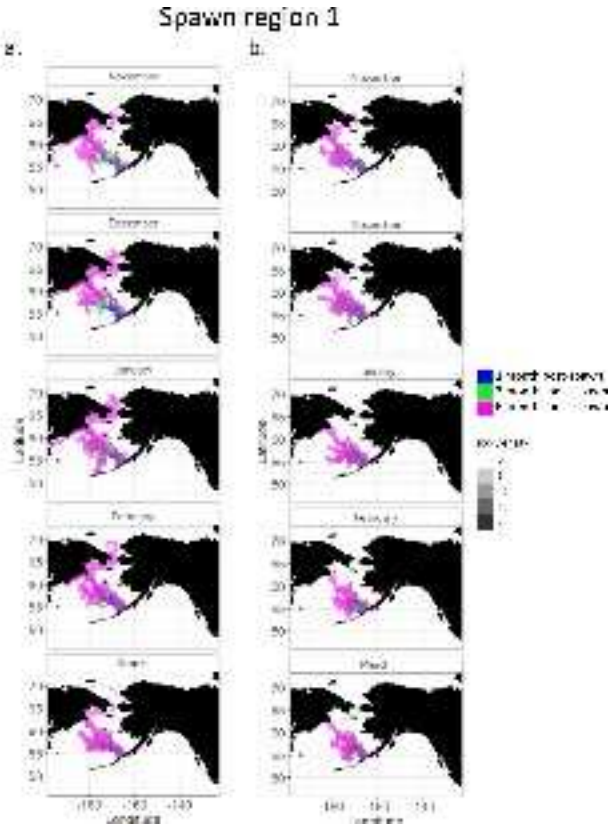

fog_12512_f4.tiff

Figure 5

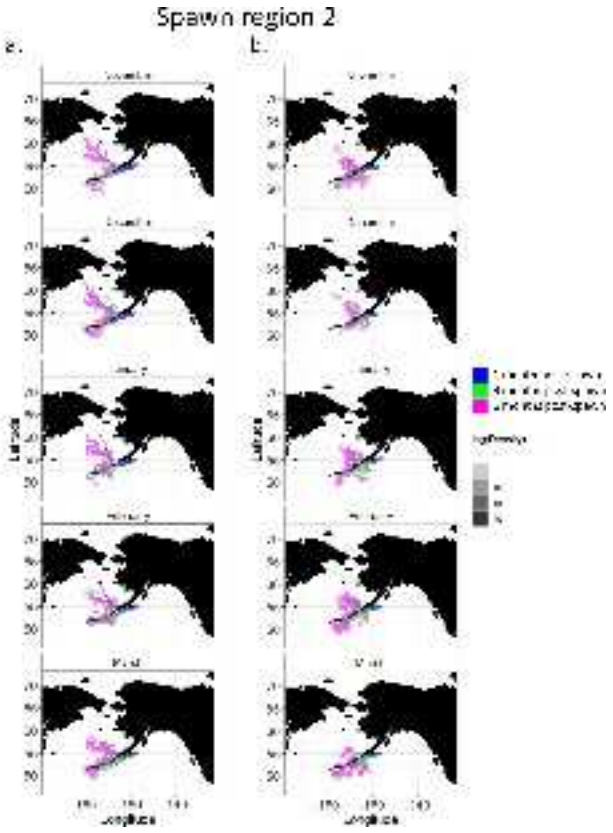

fog_12512_f5.tiff

Figure 6

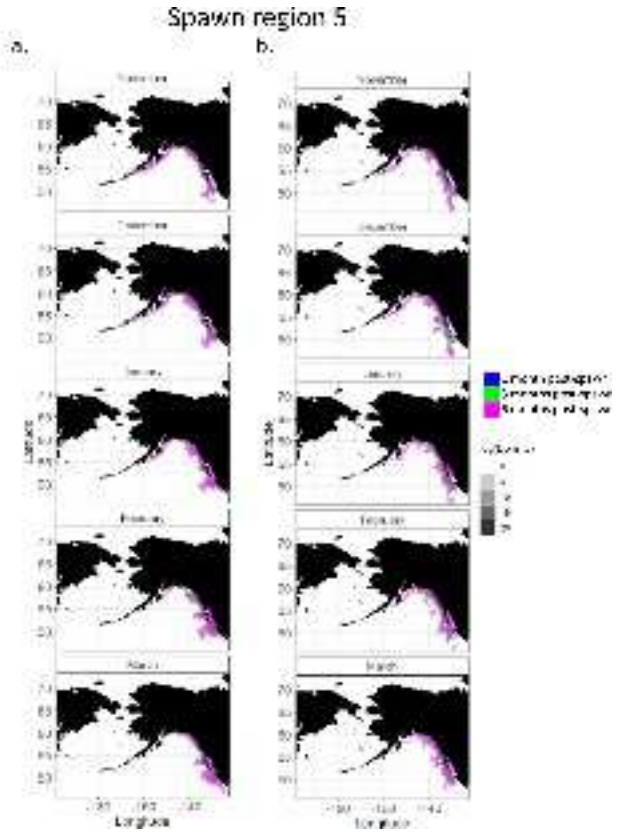

fog_12512_f6.tiff

Figure 7

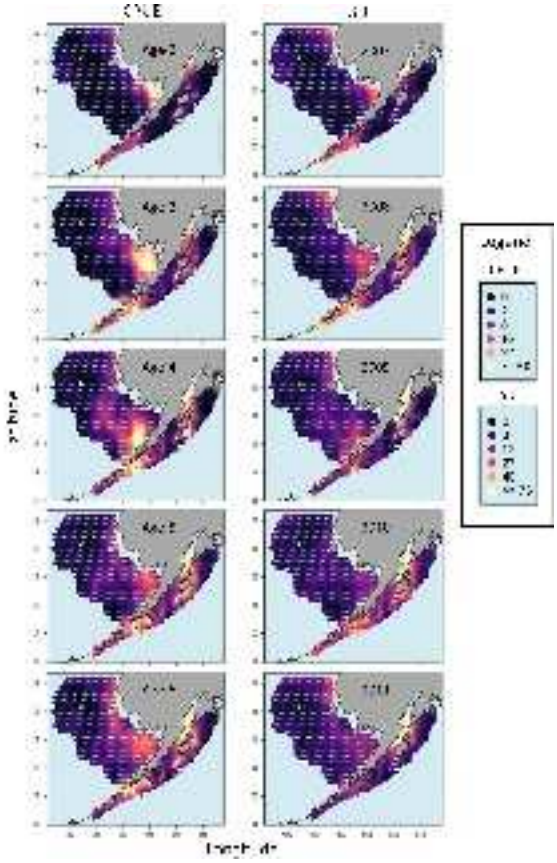

fog_12512_f7.tiff

Figure 8

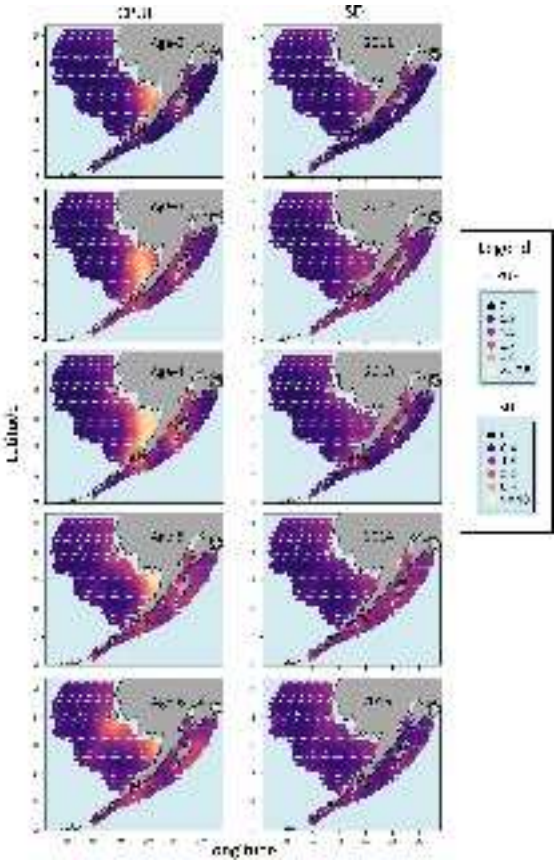

fog_12512_f8.tiff